Spectrum and Energy Efficiency Evaluation of Two-Tier Femtocell networks With Partially Open Channels

Xiaohu Ge, *Senior Member, IEEE,* Tao Han, *Member, IEEE,* Yan Zhang, *Senior Member, IEEE,* Guoqiang Mao, *Senior Member, IEEE,* Cheng-Xiang Wang, *Senior Member, IEEE,* Jing Zhang, *Member, IEEE,* Bin Yang, and Sheng Pan

Abstract—Two-tier femtocell networks is an efficient communication architecture that significantly improves throughput in indoor environments with low power consumption. Traditionally, a femtocell network is usually configured to be either completely open or completely closed in that its channels are either made available to all users or used by its own users only. This may limit network flexibility and performance. It is desirable for owners of femtocell base stations if a femtocell can partially open its channels for external users access. In such scenarios, spectrum and energy efficiency becomes a critical issue in the design of femtocell network protocols and structure. In this paper, we conduct performance analysis for two-tier femtocell networks with partially open channels. In particular, we build a Markov chain to model the channel access in the femtocell network and then derive the performance metrics in terms of the blocking probabilities. Based on stationary state probabilities derived by Markov chain models, spectrum and energy efficiency are modeled and analyzed under different scenarios characterized by critical parameters, including number of femtocells in a macrocell, average number of users, and number of open channels in a femtocell. Numerical and Monte-Carlo (MC) simulation results indicate that the number of open channels in a femtocell has an adverse impact on the spectrum and energy efficiency of two-tier femtocell networks. Results in this paper provide guidelines for trading off spectrum and energy efficiency of two-tier femtocell networks by configuring different numbers of open channels in a femtocell.

Index Terms—Femtocell networks, spectrum efficiency, energy efficiency, performance analysis, Markov chain

I. INTRODUCTION

TO accommodate the rapid increase of wireless data traffic in indoor environments, two-tier femtocell networks have been proposed to support the high spectrum efficiency in wireless communications [1], [2]. Particularly, energy efficiency in wireless communications has received lots of attention lately [3], [4]. It is important to study the spectrum and energy efficiency of femtocell networks for both economical and environmental considerations [5].

There are several studies on spectrum efficiency of femtocell networks in the literature [6]–[17]. They mainly focus on evaluating the impact of interference on the capacity and frequency reuse in wireless femtocell networks. Kim *et al.* derived the per-tier outage probability, i.e., the macrocell outage probability and the femtocell outage probability, by using a simplified mathematical model to closely approximate the femtocell interference distribution in a two-tier femtocell network [6]. Then, the capacity of the co-channel two-tier networks with outage probability constraints was obtained. Elkourdi and Simeone proposed a new approach to enable cooperations between femtocell base stations and macrocell base stations [7]. In addition, the tradeoff between the outage probability and the diversity-multiplexing gains for both uplinks and downlinks was evaluated. Zhang focused on studying the blocking probability of femtocell networks assuming completely closed channel access. The paper recommended the use of a small number of split spectrum in a femtocell to increase the service availability in a macrocell [8]. Also Pantisano *et al.* [9] adopt a closed access scheme at each femtocell to study the proposed novel framework of cooperation among femtocell users and macrocell users. Results have shown that the performance of femtocell users and macrocell users are respectively limited by interference and delay. Based on stochastic geometric techniques, the transmission success probability is derived for two cases of closed access and open access schemes at the femtocell, respectively [10]. Xiang *et al.* applied the cognitive radio technology in femtocell networks and formulated the downlink spectrum sharing problem as a

X. Ge, T. Han (corresponding author), J. Zhang, B. Yang and S. Pan are with the Department of Electronics and Information Engineering, Huazhong University of Science and Technology, Wuhan 430074, Hubei, China (email: {xhge, hantao, zhangjing, yangbin, pansheng}@mail.hust.edu.cn).

Y. Zhang is with Simula Research Laboratory, 1364 Fornebu, Norway. (email:yanzhang@ieee.org).

G. Mao is with School of Computing and Communications, University of Technology, Sydney and National ICT Australia, Sydney, Australia. (email: g.mao@ieee.org).

C.-X. Wang is with Joint Research Institute for Signal and Image Processing, School of Engineering & Physical Sciences, Heriot-Watt University, Edinburgh, EH14 4AS, UK. (email: cheng-xiang.wang@hw.ac.uk).

of open channels in a femtocell.

mixed integer nonlinear programming problem [11]. A joint channel allocation and fast power control scheme was proposed to improve the spectrum efficiency of femtocell networks [12]. Chandrasekhar and Andrews analyzed the effect of channel uncertainty on two-tier femtocell networks. The transmit power level was determined to provide the desired signal-to-interference-plus-noise ratio (SINR) for the indoor cell edge femtocell users [13]. On that basis, the beam weight was further optimized to maximize the output SINR of macrocell users and femtocell users. Sun *et al.* proposed an inter- and intra-tier interference mitigation strategy and applied the strategy to a partial co-channel assignment problem [14]. In their proposed scheme, macrocell users are divided into femto-interfering users and regular users, and then an auction-based subcarrier allocation algorithm was developed for mitigating intra-tier interference and improving the spectrum efficiency in femtocell networks. Chandrasekhar *et al.* developed a link quality protection algorithm for progressively reducing the SINR targets when a cellular user is unable to meet its SINR target in a two-tier femtocell network [15]. Jo *et al.* discovered that both the open-loop and the closed-loop control schemes can effectively compensate the uplink throughput degradation of the macrocell base station in a two-tier femtocell network [16]. Xia *et al.* evaluated both the completely open and completely closed femtocell access schemes using theoretical analysis and simulations for code division multiple access (CDMA), time division multiple access (TDMA) and orthogonal frequency division multiple access (OFDMA) scenarios [17].

Considering the low power advantage of femtocells, energy efficiency in femtocell networks has attracted attention in recent studies [18]–[26]. Particularly, Hou and Laurenson showed that the cellular and femtocell heterogeneous network architecture is able to provide a high quality of service (QoS) while significantly reduce power consumption [18]. Khirallah *et al.* proposed an approach to estimate the total energy consumption in homogeneous and heterogeneous networks with femtocell deployments [19]. Mclaughlin *et al.* proposed a power allocation strategy to optimize both spectral and energy efficiency for large-scale femtocells deployment [20]. Zhang *et al.* reported various power control and radio resource management schemes for long term evolution advanced (LTE-A) networks employing femtocells [21]. Their results demonstrated that the femtocell provides an energy efficient solution for indoor coverage in LTE-A networks. Cao and Fan validated the energy efficiency improvement by simulating a LTE femtocell networks with realistic system parameters [22]. Domenico *et al.* proposed two radio resource management schemes to enhance the energy efficiency of two-tier femtocell networks while improving both macrocell and femtocell throughput [23]. Apio *et al.* presented a switch-off algorithm to reduce the power consumption of some stations during low traffic periods in two-tier femtocell networks [24]. Ku *et al.* explored the tradeoff between the spectrum efficiency and energy efficiency in wireless networks [25]. Hong *et al.* evaluated the Energy-spectrum efficiency tradeoff in virtual MIMO

systems [26].

In this paper, we study both spectrum efficiency and energy efficiency in a two-tier femtocell network. Different from traditional studies where a femtocell is configured to be either completely open or completely closed, we allow a subset of channels to be open while the other channels to be closed in a femtocell. In particular, some femtocell channels are open for all users and the rest of femtocell channels can only be used by the femtocell's own customers. We call this channel arrangement *partially open channel arrangement*. This partially open channel arrangement is shown to be able to significantly improve network flexibility and satisfy different requirements from femtocell owners. Moreover, this *partially open channel arrangement* is valuable for trading off the spectrum and energy efficiency of two-tier femtocell networks by changing number of open channels in a femtocell. We also conduct performance analysis for two-tier femtocell networks with partially open channels based on Markov chain models. Such analysis is important to quantitatively characterize the spectrum and energy efficiency in a two-tier femtocell network. Specifically the major contributions of this paper are:

1) A Markov chain model is presented for two-tier femtocell networks with partially open channels. Furthermore, based on the stationary state probabilities of equilibrium equations in the Markov chain model, the closed-form blocking probability models of femtocell users and macrocell users are derived and analyzed.

2) Spectrum and energy efficiency models are proposed for two-tier femtocell networks with partially open channels based on the Markov chain model. Analytical results of spectrum and energy efficiency models provide guidelines for trading off the spectrum and energy efficiency of two-tier femtocell networks by configuring different numbers of open channels in a femtocell.

3) Numerical and Monte-Carlo (MC) simulation results are compared to validate the accuracy of the analysis. Moreover, simulation results demonstrate the tradeoff between spectrum efficiency and energy efficiency in two-tier femtocell networks with partially open channels.

The rest of the paper is organized as follows. Section II describes the system model of a two-tier femtocell network with partially open channels. In Section III, a Markov chain state transition diagram is proposed to model the dynamics of a femtocell. Based on the Markov chain model, the spectrum efficiency and the energy efficiency are investigated for femtocell networks with partially open channels in Section IV. Section V is the numerical results and discussions of spectrum and energy efficiency. Finally, Section VI concludes this paper.

II. Two-Tier Femtocell network System Model

Fig. 1 shows the system model of a two-tier femtocell network. A macrocell network consists of multiple macrocells that share the same bandwidth. A macrocell covers a
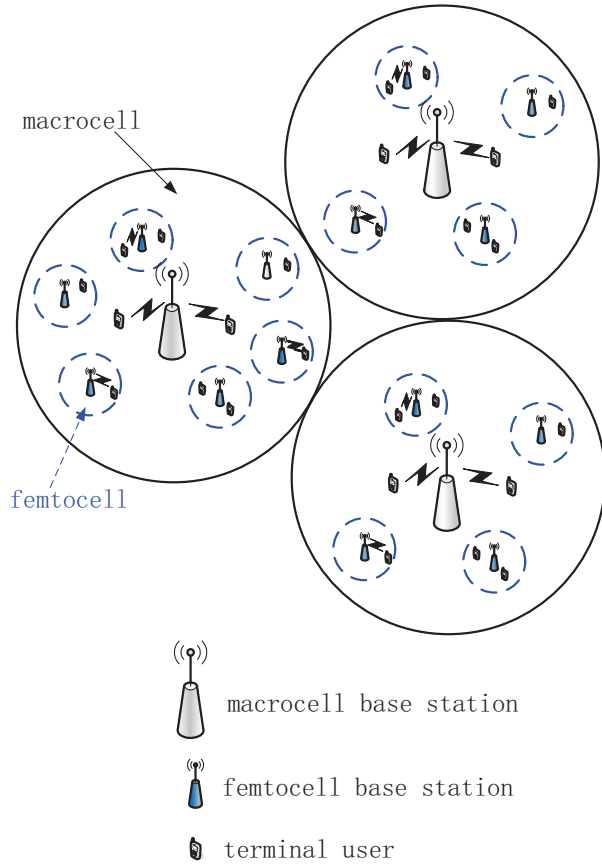
Fig. 1. Two-tier femtocell network system model.

regular circular region A_M with radius R_M and a macrocell base station (BS) is located in the center of the circle. The macrocell BS has N_M channels which are open for all users. A femtocell covers a circular region A_F with radius R_F and a femtocell BS, which is usually called as an access point (AP), is located in the center of the femtocell. A femtocell BS has N_F channels which are classified into two types: one type of channels is open in the sense that they can be used by all users; the other type of channels is called closed channels which can only be used by femtocell users. The number of open femtocell channels is denoted by N_{F_O} and the number of closed femtocell channels then becomes $N_F - N_{F\_O}$ in a femtocll.

We consider two kinds of users in the two-tier femtocell networks: macrocell users and femtocell users. Macrocell users can access all unoccupied macrocell channels and unoccupied open femtocell channels when macrocell users are located in corresponding coverage areas of these femtocells. Femtocell users can access all unoccupied macrocell channels and unoccupied femtocell channels in which these femotocell users are located. Within a specific femtocell, a femtocell user accesses the channels in the following order: a femtocell user will first access an unoccupied closed femtocell channel if there exists an unoccupied closed femtocell channel in the specific femtocell; a femtocell user will access an unoccupied open femtocell channel if all closed femtocell channels are busy and there exists an unoccupied

open femtocell channel in the specific femtocell. Finally, the femtocell user will access an unoccupied macrocell channel if all closed femtocell channels and open femtocell channels are busy in the specific femtocell. That is, a femtocell user can only access an unoccupied open femtocell channel when all closed femtocell channels are busy, and similarly for unoccupied macrocell channels. The macrocell network is overlaid with a femtocell network consisting of multiple femtocells. Femtocells do not overlap with each other. Therefore, users can hand off between a macrocell and a femtocell or between a macrocell and an adjacent macrocell. It is assumed that there are a total number of N femtocell BSs uniformly distributed within a macrocell and futhermore there are an average number of M femtocell users uniformly distributed in a femtocell. Without loss of generality, it is assumed that the traffic process originating from a user is governed by a Poisson process. Consequently, both the inter-traffic arrival time and the traffic duration follow exponential distributions. To facilitate reading, the notations and symbols used in this paper are listed in TABLE I.

III. MARKOV CHAIN MODEL OF FEMTOCELL NETWORKS

In this section, the number of occupied femtocell channels in a femtocell is first modeled by a Markov chain. By analyzing the Markov chain model, the blocking probabilities for a femtocell user and a macrocell user are derived, respectively. Furthermore, the stationary state probabilities of the Markov chain model are derived to analyze the spectrum and energy efficiency of femtocell networks in the next section.

A. Markov Chain State Transition Model

To simplify the analysis using the Markov chain model, femtocells in a macrocell are considered as a homogeneous system where all femtocells have the same equipment parameters. Furthermore, this homogeneous system is assumed to be in a statistical equilibrium, which means the average hand-off arrival rate to a femtocell is equal to the corresponding hand-off departure rate. This allows a decoupling of a femtocell from its neighbors and permits an approximate analysis by consideration the femtocell and its overlaying macrocell [27].

Let (i, j) denote the two-dimension (2-D) state of Markov chain modeling femtocell channels usage within a femtocell, where i represents the number of femtocell channels including both open femtocell channels and closed femtocell channels, used by femtocell users and j is the number of femtocell channels used by macrocell users in a femtocell. Fig. 2 illustrates the transition diagram of a femtocell. Now, we describe the state transitions in detail.

1) For $0 \leq i \leq N_F - N_{F\_O}$ and $0 \leq j \leq N_{F\_O}$, the following transitions may occur:

- $(i, j) \to (i + 1, j)$, when a closed femtocell channel is occupied by a new femtocell user call originating from a femtocell or hand-off arrival to a femtocell, where $0 \leq i < N_F - N_{F\_O}$.

TABLE I
NOTATIONS AND SYMBOLS USED IN THE PAPER

Symbol	Definition/explanation
A_M, A_F	The areas of a macrocell and a femtocell, respectively
B_w	The bandwidth of femtocell channel
G	The standard random variable with a normal distribution
I_k	The interference power received from the kth adjacent femtocell
L	The distance between the user and the corresponding femtocell BS
l	The distance between two femtocell BSs in a macrocell
M	The average number of femtocell users in a femtocell
N	The total number of femtocells within a macrocell
N_F, N_M	The number of channels in a femtocell and a macrocell, respectively
N_{F_O}	The number of open femtocell channels in a femtocell
n_0	The additive white Gaussian noise
n_w	The number of walls among femtocells in an indoor environment
P_{closed}, P_{open}	The occupancy probability of a closed femtocell channel and an open femtocell channel, respectively
P_{FU_F}, P_{MU_F}	The blocking probability of femtocell user and macrocell user in a femtocell, respectively
$P_{Handoff\_MF}$	The hand-off probability from a macrocell to a femtocell
$P_{Handoff\_FM}$	The hand-off probability from a femtocell to a macrocell
$P_{Handoff\_MM}$	The hand-off probability from a macrocell to one of adjacent macrocells
P_{U_M}	The user blocking probability in a macrocell
PW_{FBS}	The total energy consumption of femtocell BS
PW_c, PW_t	The fixed and dynamic energy consumption of femtocell BS, respectively
PW_v	The transmission power over a femtocell channel
q	The fraction of femtocell calls to the total number of calls originating from a femtocell user
R_F, R_M	The radius of a femtocell and a macrocell, respectively
R_p	the protection distance between the user and the corresponding femtocell BS
S_m	The user desired signal power
T_{cF_F}, T_{cM_F}	The channel holding time of femtocell users and macrocell users in a femtocell, respectively
T_{cF_M}, T_{cM_M}	The channel holding time of femtocell user and macrocell user in a macrocell, respectively
T_F, T_M	The traffic intensity of femtocell users and macrocell users in a macrocell, respectively
$Z_{shadowing}$	The shadowing effect in an indoor environment
α^2	The random variable is exponentially distributed with mean value 1 in a Rayleigh fading environment
β	The path loss exponent over femtocell channels
η_{EE}	The utility function of energy efficiency
λ_1, λ_2	The aggregate traffic arrival rate of femtocell users and macrocell users in a femtocell, respectively
λ_T	The total traffic arrival rate in a macrocell and its underlying N femtocells
λ_F	The new traffic arrival rate of a femtocell user
$\lambda_{FU\_F}, \lambda_{FU\_M}$	The new traffic arrival rate of femtocell users originated from a femtocell and a macrocell, respectively
λ_{FU_FM}	The new arrival rate of femtocell users in macrocell which hand off from femtocells
$\lambda_{FU\_H}, \lambda_{MU\_H}$	The total handoff-in traffic arrival rate of femtocell users and macrocell users in a femtocell, respectively
λ_{FU_H}	The total handoff traffic arrival rate from a macrocell into a femtocell by all active femtocell users
λ_{FU_MM}	The handoff traffic arrival rate of all active femtocell users from an adjacent macrocell into the macrocell
λ_M	The total traffic arrival rate of all macrocell users
$\lambda_{MU\_F}, \lambda_{MU\_M}$	The new traffic arrival rate of macrocell users originated from a femtocell and a macrocell, respectively
λ_{MU_FM}	The new arrival rate of macrocell users in macrocell which hand off from femtocells
λ_{MU_H}	The total handoff traffic arrival rate from a femtocell into a macrocell by all active macrocell users
λ_{MU_MM}	The handoff traffic arrival rate of all active macrocell users from an adjacent macrocell into the macrocell
μ_1, μ_2	The rate of channel holding time of femtocell users and macrocell users in a femtocell, respectively
σ	The deviation parameter of log-normal shadowing
$1/\eta_{RT\_F}, 1/\eta_{RT\_M}$	The average dwelling time of femtoell users and macrocell users in a femtocell, respectively
$1/\mu$	The mean of user session duration

- $(i, j) \rightarrow (i, j + 1)$, when an open femtocell channel is occupied by a new macrocell user call originating from a femtocell or hand-off arrival to a femtocell, where $0 \leq j < N_{F\_O}$.
- $(i, j) \rightarrow (i - 1, j)$, when a closed femtocell channel is released by a femtocell user call originating from a femtocell or hand-off departure from a femtocell, where $0 < i \leq N_F - N_{F\_O}$.
- $(i, j) \rightarrow (i, j - 1)$, when an open femtocell channel is released by a macrocell user call originating from a femtocell or hand-off departure from a femtocell, where $0 < j \leq N_{F\_O}$.

2) For $N_F - N_{F\_O} \leq i \leq N_F$ and $0 \leq j \leq N_F - i$, the following transitions may occur:

- $(i, j) \rightarrow (i + 1, j)$, when an open femtocell channel is occupied by a new femtocell user call originating from a femtocell or hand-off arrival to a femtocell. This event occurs when all closed femtocell channels are busy, where $N_F - N_{F\_O} \leq i < N_F$.
- $(i, j) \rightarrow (i, j + 1)$, when an open femtocell channel is occupied by a new macrocell user call originating from a femtocell or hand-off arrival to a femtocell, where $0 \leq j < N_F - i$.
- $(i, j) \rightarrow (i - 1, j)$, when an open femtocell channel is released by a femtocell user call originating from a femtocell or hand-off departure from a femtocell. This event occurs when the femtocell user call has occupied an open femtocell channel, where $N_F - N_{F\_O} < i \leq N_F$.
- $(i, j) \rightarrow (i, j - 1)$, when an open femtocell channel is released by a macrocell user call originating from a femtocell or hand-off departure from a femtocell, where
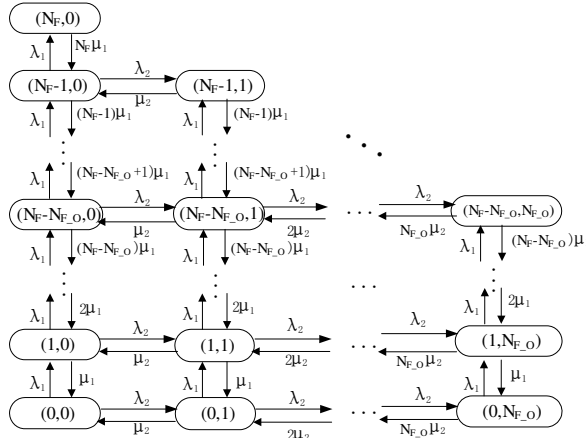
Fig. 2. State transition diagram in a femtocell.

$$0 < j \le N_F - i.$$

B. Analysis of the Markov Chain Model

In Fig. 1, we term a macrocell and its underlying N femtocells as an entity and assume that the total originating traffic process in an entity follows a Poisson process with an arrive rate λ_T. For a femtocell user, it may generate both indoor, i.e., femtocell, and outdoor, i.e., macrocell, call activities though indoor call activities occur more frequently. The fraction of indoor calls to the total number of calls originating from a femtocell user is denoted as q and the new traffic arrival rate of a femtocell user is denoted by λ_F. Hence, the total traffic arrival rate of all macrocell users in an entity is $\lambda_M = \lambda_T - NM\lambda_F$. The total traffic arrival rate of all macrocell users in a femtocell is $\frac{A_F}{A_M} \cdot \lambda_M$ and the total traffic arrival rate of all macrocell users in a macrocell is $\left(1 - N\frac{A_F}{A_M}\right)\lambda_M$. The user session duration, which refers to the time duration of a requested session connection, is assumed to be an exponential distribution with mean $1/\mu$. A user dwelling time refers to the time duration a user stays in a cell. The femtocell users and macrocell users dwelling time in a femtocell are assumed to follow an exponential distribution with mean $1/\eta_{RT\_F}$ and $1/\eta_{RT\_M}$, respectively.

The aggregate traffic arrival rate of femtocell users λ_1 in a femtocell is divided into two parts. One part is the new traffic arrival rate of femtocell users λ_{FU_F} originating from a femtocell and the other part is the total handoff-in traffic arrival rate of femtocell users λ_{FU_H} caused by handoff from a macrocell into a femtocell by active femtocell users. Therefore, the aggregate traffic arrival rate of femtocell users λ_1 is determined by

$$\lambda_1 = \lambda_{FU\_F} + \lambda_{FU\_H}. \tag{1}$$

Moreover, the new traffic arrival rate of femtocell users λ_{FU_F} originating from a femtocell is given by

$$\lambda_{FU\_F} = Mq\lambda_F. \tag{2}$$

Let P_{U_M} and P_{FU_F} denote the user blocking probability in a macrocell and the blocking probability of femtocell

users in a femtocell, respectively. Based on the results in (2) and Appendix A, the aggregate traffic arrival rate of femtocell users λ_1 is derived as follows

$$\lambda_1 = Mq\lambda_F + \frac{1}{N}\left(\lambda_{FU\_M} + \lambda_{FU\_FM} + \lambda_{FU\_MM}\right) \\ \cdot (1 - P_{U\_M}) \cdot P_{Handoff\_MF}, \tag{3a}$$

with

$$\lambda_{FU\_M} = NM(1 - q) \cdot \lambda_F, \tag{3b}$$

$$\lambda_{FU\_FM} = N\lambda_1 \cdot (1 - P_{FU\_F}) \cdot P_{Handoff\_FM}, \tag{3c}$$

$$\lambda_{FU\_MM} = (\lambda_{FU\_M} + \lambda_{FU\_FM} + \lambda_{FU\_MM}) \\ \cdot (1 - P_{U\_M}) \cdot P_{Handoff\_MM}. \tag{3d}$$

The channel holding time of femtocell users T_{cF_F} with rate μ_1 in a femtocell is the minimum of the session duration and the average femtocell users dwelling time, i.e., $T_{cF\_F} = min(1/\mu, 1/\eta_{RT\_F})$. Then μ_1 is given by [28]

$$\mu_1 = \mu + \eta_{RT\_F}. \tag{4}$$

The aggregate traffic arrival rate of macrocell users λ_2 in a femtocell is also divided into two parts. One part is the new traffic arrival rate of macrocell users λ_{MU_F} originating from femtocell itself and the other part is the handoff-in traffic arrival rate of macrocell users λ_{MU_H} caused by handoff from a macrocell into a femtocell by active macrocell users. Therefore, the aggregate traffic arrival rate of macrocell users λ_2 in a femtocell is calculated by

$$\lambda_2 = \lambda_{MU\_F} + \lambda_{MU\_H}. \tag{5}$$

Moreover, the new traffic arrival rate of macrocell users λ_{MU_F} is given by

$$\lambda_{MU\_F} = \frac{A_F}{A_M}\lambda_M. \tag{6}$$

Let P_{MU_F} denote the blocking probability of macrocell user in a femtocell. Based on the results in (6) and Appendix B, the aggregate traffic arrival rate of macrocell users λ_2 is derived as follows

$$\lambda_2 = \frac{A_F}{A_M}\lambda_M + \frac{1}{N}\left(\lambda_{MU\_M} + \lambda_{MU\_FM} + \lambda_{MU\_MM}\right) \\ \cdot (1 - P_{U\_M}) \cdot P_{Handoff\_MF}, \tag{7a}$$

with

$$\lambda_{MU\_M} = \left(1 - N\frac{A_F}{A_M}\right) \cdot \lambda_M, \tag{7b}$$

$$\lambda_{MU\_FM} = N\lambda_2 \cdot (1 - P_{MU\_F}) \cdot P_{Handoff\_FM}, \tag{7c}$$

$$\lambda_{MU\_MM} = (\lambda_{MU\_M} + \lambda_{MU\_FM} + \lambda_{MU\_MM}) \\ \cdot (1 - P_{U\_M}) \cdot P_{Handoff\_MM}. \tag{7d}$$

The channel holding time of macrocell users T_{cM_F} with rate μ_2 in a femtocell is the minimum of the session duration and the average macrocell users dwelling time, i.e., $T_{cM\_F} = min(1/\mu, 1/\eta_{RT\_M})$. Therefore, μ_2 is given by [28]

$$\mu_2 = \mu + \eta_{RT\_M}. \tag{8}$$

$$\begin{cases} (\lambda_1 + \lambda_2 + \mu_1 i + \mu_2 j) S(i,j) = (i+1)\mu_1 S(i+1,j) \\ \quad + (j+1)\mu_2 S(i,j+1) + \lambda_1 S(i-1,j) + \lambda_2 S(i,j-1), 0 \le i \le N_F, 0 \le j \le \min(N_{F\_O}, N_F - i) \\ (\lambda_1 + \lambda_2 + \mu_1 i + \mu_2 j) S(i,j) = (i+1)\mu_1 S(i+1,j) + (j+1)\mu_2 S(i,j+1) \\ \quad + \lambda_2 S(i,j-1), i = 0 \\ (\lambda_1 + \lambda_2 + \mu_1 i + \mu_2 j) S(i,j) = (i+1)\mu_1 S(i+1,j) + (j+1)\mu_2 S(i,j+1) \\ \quad + \lambda_1 S(i-1,j), j = 0 \\ (\lambda_1 + \mu_1 i + \mu_2 N_{F\_O}) S(i,j) = (i+1)\mu_1 S(i+1,j) + \lambda_1 S(i-1,j) \\ \quad + \lambda_2 S(i,j-1), j = N_{F\_O} \\ (\mu_1 i + \mu_2(N_F - i)) S(i,j) = +\lambda_1 S(i-1,j) + \lambda_2 S(i,j-1), i+j = N_F \end{cases} , \quad (9)$$

$$E(T_{cM\_M}) = \frac{1}{\mu + \eta_{RT\_M}} \left[N\frac{A_F}{A_M} \cdot P_{MU\_F} + \left(1 - N\frac{A_F}{A_M}\right) \right] + N\frac{A_F}{A_M}(1 - P_{MU\_F}) \cdot E(Z), \quad (16a)$$

$$E(Z) = \frac{1}{\mu} - \frac{1}{\mu} \left[\frac{\ln\left(\frac{\mu}{\eta_{RT\_M}}\right)}{\frac{\mu}{\eta_{RT\_M}}} - \frac{\eta_{RT\_M}}{\mu}\left(e^{-\frac{\eta_{RT\_M}}{\mu}} - 1\right) \right], \quad (16b)$$

$$E(T_{cF\_M}) = \frac{1}{\mu + \eta_{RT\_M}} \left[N\frac{A_F}{A_M} \cdot P_{FU\_F} + \left(1 - N\frac{A_F}{A_M}\right) \right] + N\frac{A_F}{A_M}(1 - P_{FU\_F}) \cdot E(Z). \quad (18)$$

Based on the Markov chain state transition diagram in Fig. 2, the set of equilibrium equations is given by (9), where $S(i,j)$ is the stationary state probability of Markov chain modeling femtocell channels in a femtocell. After solving (9), a closed-form expression of the state probability $S(i,j)$ is given by

$$S(i,j) = \frac{(\lambda_1/\mu_1)^i (\lambda_2/\mu_2)^j}{i!j!} S(0,0). \quad (10)$$

The normalization condition is given by

$$\sum_{(i,j)} S(i,j) = 1. \quad (11)$$

From (11), the idle-state probability $S(0,0)$, i.e. the probability that there is no active user using the channel, is derived as follows

$$S(0,0) = \left\{ \sum_{i=0}^{N_F} \sum_{j=0}^{j=\min(N_{F\_O}, N_F - i)} \frac{(\lambda_1/\mu_1)^i (\lambda_2/\mu_2)^j}{i!j!} \right\}^{-1}. \quad (12)$$

As a consequence of the above equation, all other state probabilities can be obtained by substituting (12) into (10).

Note that the focus of this paper is on studying the call blocking probability where an incoming call is blocked when there is no channel available in the network to serve the call. Based on the Markov chain state transition diagram in Fig. 2 and (10), the blocking probability of femtocell user in a femtocell is given by

$$P_{FU\_F} = \sum_{i=N_F - N_{F\_O}}^{i=N_F} S(i, N_F - i). \quad (13)$$

Moreover, the blocking probability of macrocell user in a

femtocell is given by

$$P_{MU\_F} = \sum_{i=0}^{i=N_F - N_{F\_O} - 1} S(i, N_{F\_O}) + \sum_{i=N_F - N_{F\_O}}^{i=N_F} S(i, N_F - i). \quad (14)$$

Based on the Erlang-B formula in [29], the user blocking probability in a macrocell is given by

$$P_{U\_M} = \frac{(T_M + T_F)^{N_M}/N_M!}{\sum_{k=0}^{N_M} (T_M + T_F)^k/k!}, \quad (15)$$

where T_M and T_F are traffic intensities of macrocell users and femtocell users in a macrocell, respectively. N_M is the number of channels in a macrocell. Let T_{cM_M} denotes the channel holding time of a macrocell user in a macrocell. It can be readily shown that the expectation of T_{cM_M} is given by (16) [8], where $E[\cdot]$ denotes an expectation operator. Then, the traffic intensity of macrocell users T_M in a macrocell is calculated by

$$T_M = (\lambda_{MU\_M} + \lambda_{MU\_FM} + \lambda_{MU\_MM}) \cdot E(T_{cM\_M}). \quad (17)$$

Let T_{cF_M} denotes the channel holding time of a femtocell user in a macrocell. The expectation of T_{cF_M} is given by (18) [8].

Furthermore, the traffic intensity of femtocell user T_F in a macrocell is given by

$$T_F = (\lambda_{FU\_M} + \lambda_{FU\_FM} + \lambda_{FU\_MM}) \cdot E(T_{cF\_M}). \quad (19)$$

Substituting (17) and (19) into (15), a closed-form user blocking probability in a macrocell is derived. Equations (13), (14) and (15) represent a nonlinear system, which can be solved by numerical techniques.

C. Analysis of blocking probabilities

Based on the proposed blocking probability models for two-tier femtocell networks, performance evaluation is analyzed as follows. Unless otherwise specified, the key parameters are configured as: $R_M = 1000m$, $R_F = 20m$, $N = 40$, $N_F = 3$, $N_{F\_O} = 1$, $N_M = 24$, $q = 0.6$, $\lambda_F = 0.002$ and M is 4, 6 and 8 [30], [31]. The average value of the user session duration is set as $1/\mu = 110$ seconds [32]. The average values of femtocell users and macrocell users dwelling time in a femtocell are configured as $1/\eta_{RT\_F} = 990$ and $1/\eta_{RT\_M} = 300$ seconds [8], [11], respectively. To validate the proposed model, we compare the proposed model with the model derived from the reference [8] in Fig. 3 and Fig. 4.

Fig. 3 shows the user blocking probability P_{U_M} in a macrocell in terms of the total arrival rate λ_T with different average number of femtocell users in a femtocell. The curves in Fig. 3 illustrate that the value of P_{U_M} increases with an increase in the arrival rate λ_T. When the number of occupied channels increases as a consequence of an increase in the arrival rate in a macrocell, the user blocking probability in a macrocell P_{U_M} increases. When the total arrival rate λ_T is fixed, it is interesting to see that the user blocking probability P_{U_M} decreases with an increase in the average number of femtocell users in a femtocell. This is caused by that an increase in the average number of femtocell users in a femtocell will reduce the traffic flow density in a macrocell when the total arrival rate λ_T is fixed. As a consequence, the user blocking probability P_{U_M} decreases when more users are added into a femtocell. The curves obtained from the proposed model exhibit a good match with the curves obtained from the model in reference [8]. This result indicates that the proposed model is consistent with the model in reference [8] if the impact of closed and open femtocell channels is not considered in simulation results.

Fig. 4 illustrates the blocking probability of femtocell users P_{FU_M} in terms of the total arrival rate λ_T with different average number of femtocell users in a femtocell. The curves in Fig. 4 show that the blocking probability of femtocell users P_{FU_M} increases with the higher total arrival rate λ_T. We can also observe that, when the total arrival rate λ_T is fixed, the blocking probabilities of femtocell users increase with an increase in the average number of femtocell users. Compared with the curves obtained from the model in reference [8], the curves obtained from the proposed model demonstrate the same trend in Fig. 4. In the proposed model, femtocell channels are not only open for femtocell users but also partially open to macrocell users. In the model derived from [8], femtocell channels are only open for femtocell users. In this case, the blocking probability derived from the proposed model is higher than the blocking probability in [8].

Fig. 5 analyzes the blocking probability of macrocell users P_{MU_M} in terms of the total arrival rate λ_T with different average number of femtocell users in a femtocell. Numerical results show that the blocking probability of macrocell users P_{MU_M} increases with the higher total arrival rate λ_T. Moreover, when the total arrival rate λ_T is
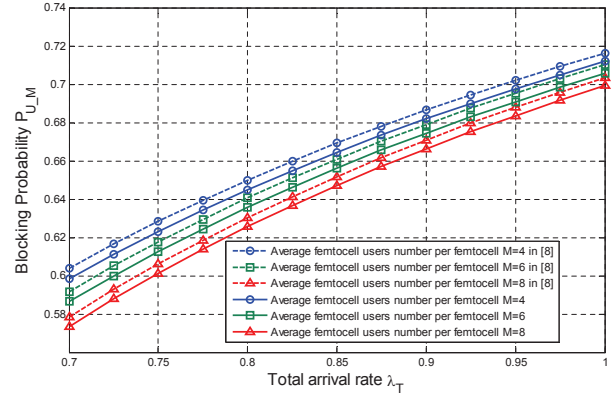

Fig. 3. The user blocking probability in terms of total arrival rate with different average number of femtocell users.
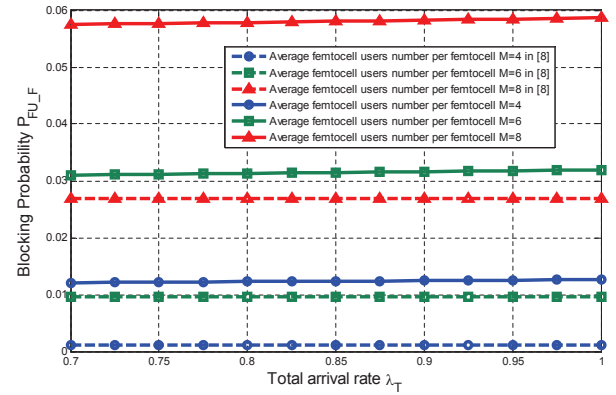

Fig. 4. The blocking probability of femtocell users in terms of total arrival rate with different average number of femtocell users.

fixed, the blocking probability of macrocell users increases with an increase in the average number of femtocell users in a femtocell.
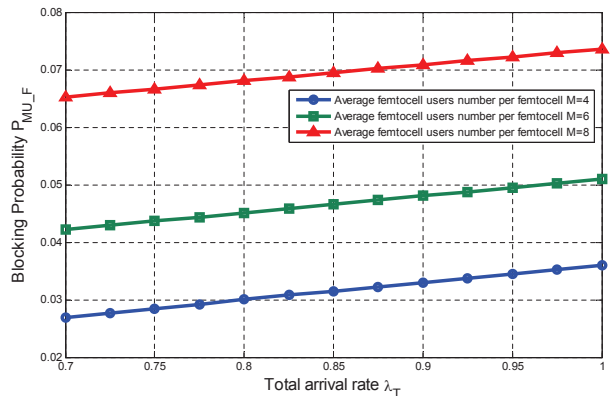

Fig. 5. The blocking probability of macrocell users in terms of total arrival rate with different average number of femtocell users.

IV. Spectrum and Energy Efficiency Models of Femtocell Networks

Based on the stationary state probabilities derived by the Markov chain models, the spectrum and energy efficiency models are proposed for femtocell networks. Furthermore, simulations are performed to analyze the performance parameters of spectrum and energy efficiency in femtocell networks.

A. Spectrum Efficiency Model of Femtocell Networks

The occupancy probability of a closed femtocell channel is analyzed by considering two situations separately. In the first situation, the number of channels occupied by femtocell users is smaller than or equal to the number of closed femtocell channels in a femtocell; in the second situation, the number of channels occupied by femtocell users is larger than the number of closed femtocell channels in a femtocell. Therefore, using (10), the occupancy probability of a closed femtocell channel is given by

$$
\begin{aligned}
P_{closed} = & \sum_{i=1}^{N_F - N_{F\_O}} \sum_{j=0}^{N_{F\_O}} \frac{\binom{N_F - N_{F\_O} - 1}{i-1}}{\binom{N_F - N_{F\_O}}{i}} S(i,j) \\
& + \sum_{i=N_F - N_{F\_O}+1}^{N_F} \sum_{j=0}^{N_F - i} S(i,j),
\end{aligned}
\tag{20}
$$

where $\binom{x}{y}$ is the binomial coefficients with parameters x and y. Similarly, the occupancy probability of an open femtocell channel can also be analyzed by considering two situations separately. The first situation occurs when the femtocell users do not occupy the open femtocell channels in a femtocell. The second situation occurs when the femtocell users occupy the open femtocell channels in a femtocell. Therefore, using (10), the occupancy probability of an open femtocell channel is given by

$$
\begin{aligned}
P_{open} = & \sum_{i=0}^{N_F - N_{F\_O}} \sum_{j=1}^{N_{F\_O}} \frac{\binom{N_{F\_O} - 1}{j-1}}{\binom{N_{F\_O}}{j}} S(i,j) \\
& + \sum_{i=N_F - N_{F\_O}+1}^{N_F} \sum_{j=0}^{N_F - i} \frac{\binom{N_{F\_O} - 1}{i-(N_F - N_{F\_O})-1}}{\binom{N_{F\_O}}{i-(N_F - N_{F\_O})}} S(i,j),
\end{aligned}
\tag{21}
$$

Considering that femtocells are assumed to be uniformly distributed in a macrocell, the probability density function (PDF) of the distance l between two femtocell BSs in a macrocell is given [33]

$$
f(l) = \frac{4l}{\pi R_M^2} \left(\arccos\left(\frac{l}{2R_M}\right) - \frac{l}{2R_M}\sqrt{1 - \left(\frac{l}{2R_M}\right)^2} \right)
\tag{22}
$$

where $0 \le l \le 2R_M$. Moreover, considering that the distance between a user and its associated femtocell BS is usually small, the distance between a user and the interfering femtocell BS is approximated by the distance between the associated femtocell BS and the interfering femtocell BS.

To avoid co-channel interference between macrocells and femtocells, it is assumed that macrocells and femtocells use different frequencies for communications. Furthermore,

all femtocells in a macrocell share the same frequency bandwidth and the frequency bandwidth used by a femtocell is divided into N_F no-overlapping sub-bandwidth. Here, each frequency sub-bandwidth corresponds to a femtocell channel. In this case, the number of interfering users from adjacent femtocells is no more than the number of femtocells in a macrocell. For the sake of illustration, the number of interfering users from an adjacent femtocell is configured as one. Since the radius of a macrocell is much larger than the radius of a femtocell, the co-channel interference from adjacent macrocells is ignored in this paper. Furthermore, a user in a femtocell is only interfered by users using same frequency sub-bandwidth in adjacent femtocells and located in the same macrocell. We consider the propagation effects of path loss, shadowing, and Rayleigh fading over femtocell channels. When an active user is located in a femtocell, the active user receives interference from the kth adjacent femtocell, $1 \le k \le N-1$. The interference power originating from the kth adjacent femtocell is expressed as [34]–[36]

$$
I_k = PW_v \frac{e^{2\sigma G}\alpha^2}{10^{1.2n_w}l^\beta},
\tag{23}
$$

where PW_v is the transmission power over a femtocell channel. The total transmission power of a femtocell is distributed over all femtocell channels. The term $e^{2\sigma G}$ accounts for log-normal shadowing with deviation σ, where $G \sim Gaussian(0,1)$ represents a standard normal random variable. The random variable α^2 is exponentially distributed with mean value 1 in a Rayleigh fading environment. The item $10^{1.2n_w}$ refers to the through-wall loss in an indoor environment with the number of walls among femtocells n_w. The item l^β stands for the path loss effect between two femtocells within a macrocell with path loss exponent β.

Considering that femtocells are usually used for indoor environment, the signal received by a user in a femtocell does not consider the small scale fading and the through-wall loss. Therefore, the desired signal power S_m received by the mth user in a femtocell is given by

$$
S_m = PW_v \frac{Z_{shadowing}}{L^\beta},
\tag{24}
$$

where $Z_{shadowing}$ indicates the shadowing effect in an indoor environment and is assumed to be 4dB [37]. L denotes the distance between the user UE_m and the corresponding femtocell BS. Users are uniformly distributed in a femtocell and the protection distance between the user and the corresponding femtocell BS is R_p. The PDF of L is given by

$$
f(L) = \frac{2L}{R_F^2}
\tag{25}
$$

where $R_p \le L \le R_F$.

Furthermore, the capacity of all closed channels in a femtocell is derived by (26), where n_0 denotes the additive white Gaussian noise (AWGN) in wireless channels. B_W represents the bandwidth of femtocell channel. The capacity of all open channels in a femtocell is derived by (27). As a consequence, the total capacity of a femtocell is derived by (28).

$$C_{closed} = \sum_{m=1}^{N_F - N_{F\_O}} B_W \log \left(1 + \frac{P_{closed} S_m}{n_0 + \sum_{n=1}^{N-1} \binom{N-1}{n} \left(\frac{P_{closed}}{N_F - N_{F\_O}} \right)^n \left(1 - \frac{P_{closed}}{N_F - N_{F\_O}} \right)^{N-1-n} \sum_{k=1}^{n} I_k} \right),$$ (26)

$$C_{open} = \sum_{m=1}^{N_{F\_O}} B_W \log \left(1 + \frac{P_{open} S_m}{n_0 + \sum_{n=1}^{N-1} \binom{N-1}{n} \left(\frac{P_{open}}{N_{F\_O}} \right)^n \left(1 - \frac{P_{open}}{N_{F\_O}} \right)^{N-1-n} \sum_{k=1}^{n} I_k} \right).$$ (27)

$$C_{total} = C_{closed} + C_{open} = \sum_{m=1}^{N_F - N_{F\_O}} B_W \log \left(1 + \frac{P_{closed} S_m}{n_0 + \sum_{n=1}^{N-1} \binom{N-1}{n} \left(\frac{P_{closed}}{N_F - N_{F\_O}} \right)^n \left(1 - \frac{P_{closed}}{N_F - N_{F\_O}} \right)^{N-1-n} \sum_{k=1}^{n} I_k} \right)$$
$$+ \sum_{m=1}^{N_{F\_O}} B_W \log \left(1 + \frac{P_{open} S_m}{n_0 + \sum_{n=1}^{N-1} \binom{N-1}{n} \left(\frac{P_{open}}{N_{F\_O}} \right)^n \left(1 - \frac{P_{open}}{N_{F\_O}} \right)^{N-1-n} \sum_{k=1}^{n} I_k} \right)$$ (28)

$$\eta_{EE} = \frac{PW_c + \sum_{i=0}^{N_F} \sum_{j=0}^{\min(N_{F\_O}, N_F - i)} (i+j) S(i,j) PW_v}{C_{total}},$$ (32a)

$$C_{total} = \sum_{m=1}^{N_F - N_{F\_O}} B_W \log \left(1 + \frac{P_{closed} S_m}{n_0 + \sum_{n=1}^{N-1} \binom{N-1}{n} \left(\frac{P_{closed}}{N_F - N_{F\_O}} \right)^n \left(1 - \frac{P_{closed}}{N_F - N_{F\_O}} \right)^{N-1-n} \sum_{k=1}^{n} I_k} \right)$$
$$+ \sum_{m=1}^{N_{F\_O}} B_W \log \left(1 + \frac{P_{open} S_m}{n_0 + \sum_{n=1}^{N-1} \binom{N-1}{n} \left(\frac{P_{open}}{N_{F\_O}} \right)^n \left(1 - \frac{P_{open}}{N_{F\_O}} \right)^{N-1-n} \sum_{k=1}^{n} I_k} \right)$$ (32b)

B. Energy Efficiency Model of Femtocell Networks

A femtocell BS energy consumption can be decomposed into the fixed energy consumption part and the dynamic energy consumption part [3]. The fixed energy consumption, e.g., the circuit energy consumption, is the baseline energy consumed at a femtocell BS. The circuit energy consumption usually depends on both hardware and software configurations of a femtocell BS and is independent of the number of occupied channels. The dynamic energy consumption accounts for the transmission energy consumed in radio frequency (RF) transmission circuits depending on the number of occupied channels. As an easy consequence of the above analysis, we can build a femtocell BS energy consumption model

$$E\left(PW_{FBS}\right) = PW_c + E\left(PW_t\right),$$ (29)

where PW_{FBS} denotes the total energy consumption of femtocell BS. PW_c refers to the fixed energy consumption of femtocell BS. PW_t indicates the dynamic energy consumption of femtocell BS. The dynamic energy consumption is mainly associated with the transmission energy over wireless channels. Based on the Markov chain state transition diagram in Fig. 2, the average dynamic energy consumption is derived as follows

$$E\left(PW_t\right) = \sum_{i=0}^{N_F} \sum_{j=0}^{\min(N_{F\_O}, N_F - i)} (i+j) S(i,j) PW_v.$$ (30)

It is very important to study the spectrum and energy

efficiency from a systematic perspective. For this, we introduce a new performance metric *the utility function of energy efficiency*, which is defined as the ratio of the total capacity in a femtocell to the average total energy consumption in a femtocell BS. Let η_{EE} denote the utility function of energy efficiency. Then, we have

$$\eta_{EE} = \frac{E\left(PW_{FBS}\right)}{C_{total}}.$$ (31)

Based on (28) and (29), the energy efficiency model can be further derived as follows (32).

V. NUMERICAL RESULTS AND DISCUSSIONS

In this subsections numerical and MC simulations are presented to demonstrate interactions between the femtocell energy efficiency metrics and critical performance-impacting parameters. Unless otherwise specified, the following parameters are used in the numerical and MC simulations: $\sigma = 8dB$, $\beta = 2$, $n_w = 2$, and $R_p = 5m$.

First, we fix the number of total femtocell channels $N_F = 6$ and the number of open femtocell channels $N_{F\_O} = 3$. Fig. 6 illustrates the spectrum efficiency of the femtocell networks in terms of the average number of femtocells users with different number of femtocells in a macrocell, in which "Num" labels the numerical results and "MC" represents the MC simulation results. When the number of femtocells in a macrocell is fixed, the spectrum efficiency increases with an increase in the average number of users in a femtocell. When the average number of users

in a femtocell is fixed, the spectrum efficiency of femtocell networks decreases with an increase in the number of femtocells in a macrocell. Fig. 7 shows the energy efficiency of the femtocell networks in terms of the average number of femtocell users with different number of femtocells in a macrocell. When the number of femtocells in a macrocell is fixed, the energy efficiency of femtocell networks increases with an increase in the average number of users in a femtocell. When the average number of users in a femtocell is fixed, the energy efficiency of femtocell networks increases with an increase in the number of femtocells in a macrocell. Compared with results from MC simulations, these numerical results are validated in Fig. 6 and Fig. 7, which demonstrate good accuracy of the results.

Secondly, we fix the number of open femtocell channels $N_{F\_O} = 3$ and the average number of users as 4 in a femtocell. Fig. 8 shows the spectrum efficiency in terms of the number of closed channels in a femtocell with different number of femtocells in a macrocell. It is observed that the spectrum efficiency increases with an increase in the number of closed channels in a femtocell. In addition, when the number of closed channels is fixed, the spectrum efficiency of the femtocell networks decreases with an increase in the number of femtocells in a macrocell. Fig. 9 shows the energy efficiency performance in terms of the number of closed channels in a femtocell. We can observe that the energy efficiency of the femtocell networks decreases with an increase in the number of closed channels in a femtocell. On the other hand, the energy efficiency increases with an increase in the number of femtocells in a macrocell. The numerical results are validated by the MC simulation results shown in Fig. 8 and Fig. 9. However, the MC simulation curves are less than the numerical curves in Fig. 8 and Fig. 9. Considering that the MC simulation results are realized by finite simulation calculations, a few MC simulation calculation values with small probabilities will be discarded in the final results.

In the end, we fix the number of closed femtocell channels to be 2 and the number of femtocells in a macrocell to be 25 for the following simulation. Fig. 10 shows the spectrum efficiency of the femtocell networks in terms of the average number of femtocell users with different number of open channels in a femtocell. In this example, the number of total channels in a femtocell is set as 8. We can see that the spectrum efficiency of the femtocell networks increases with an increase in the average number of users in a femtocell. When the average number of users is fixed in a femtocell, the spectrum efficiency increases with an increase in the number of open channels in a femtocell. Fig. 11 shows the energy efficiency of the femtocell networks in terms of the average number of femtocell users with different open channels in a femtocell. The curves show that the energy efficiency increases with an increase in the average number of users in a femtocell and the energy efficiency decreases with an increase in the number of open channels in a femtocell. According to the energy efficiency model in (32), the average dynamic energy consumption linearly increases with an increase in the number of open femtocell channels
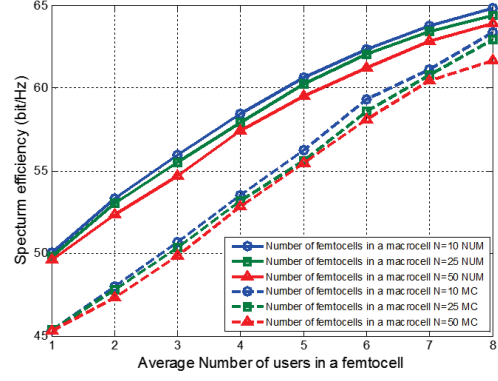

Fig. 6.　Spectrum efficiency of femtocell networks with respect to the average number of users in a femtocell.
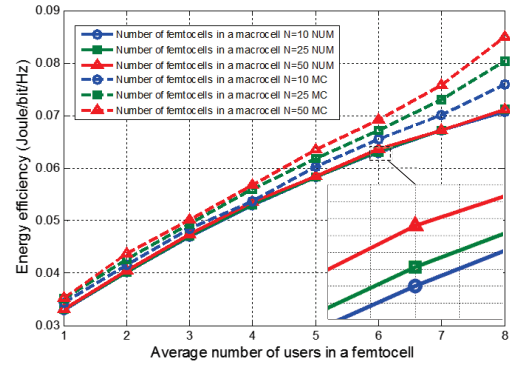

Fig. 7.　Energy efficiency of femtocell networks with respect to the average number of users in a femtocell.

but the total capacity of a femtocell only increases logarithmically with an increase in the number of open femtocell channels. Therefore, when the number of open femtocell channels increases, the energy efficiency decreases. Based on results of Fig. 8-11, our analytical models and simulation results indicate that an increase in the number of open or closed femtocell channels can conduce to the increase of spectrum efficiency and the decrease of energy efficiency in a two-tier femtocell networks. As a consequence, the results provide guidelines for trading off the spectrum and energy efficiency of two-tier femtocell networks by configuring different number of open or closed femtocell channels in a femtocell.

VI. CONCLUSIONS

In this paper, the channel occupancy in a femtocell is modeled by Markov chains. To derive state transition probabilities in a femtocell, a Markov chain state transition diagram for a femtocell is presented. Moreover, the user blocking probability in a macrocell and the blocking probabilities of femtocell and macrocell users in a femtocell are derived and analyzed. Furthermore, spectrum and
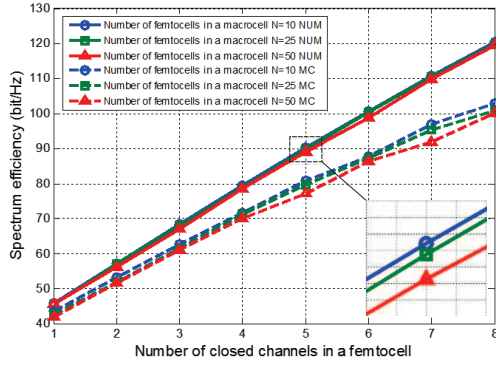
Fig. 8. Spectrum efficiency of femtocell networks with respect to the number of closed channels in a femtocell.
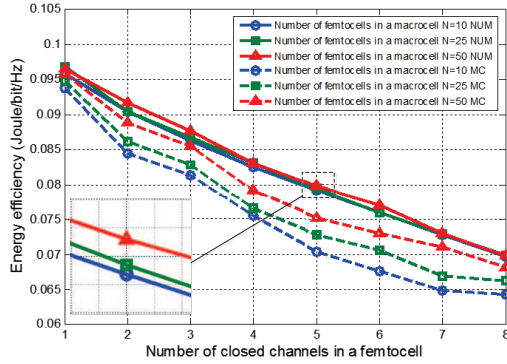

Fig. 9. Energy efficiency of femtocell networks with respect to the number of closed channels in a femtocell.
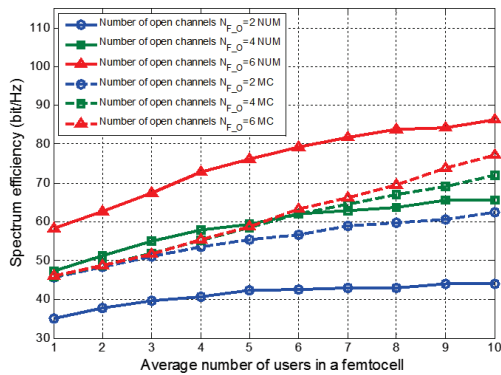

Fig. 10. Spectrum efficiency of femtocell networks with respect to the number of open channels.
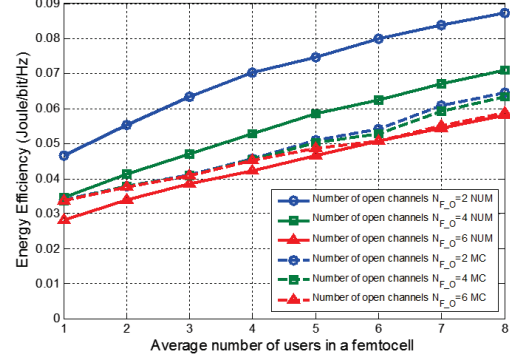

Fig. 11. Energy efficiency of femtocell networks with respect to the number of open channels.

energy efficiency models are proposed for two-tier femtocell networks with partially open channels. Simulation results have shown the impacts of critical parameters on the two-tier femtocell networks, including the number of femtocell users, the number of femtocells in a macrocell, and the number of open or closed channels in a femtocell. Our analysis indicates that the spectrum and energy efficiency of two-tier femtocell networks can be traded off by configuring different numbers of open channels in a femtocell. Moreover, the results of energy efficiency for two-tier femtocell networks can provide useful guidelines to determine the number of femtocells to deploy in a macrocell.

APPENDIX A

The handoff probability from a femtocell into a macrocell is defined as $P_{Handoff\_FM}$, which is given by [8]

$$P_{Handoff\_FM} = \frac{\eta_{RT\_F}}{\mu + \eta_{RT\_F}}. \tag{33}$$

The handoff probability from a macrocell into a femtocell is defined as $P_{Handoff\_MF}$, which is given by (34) [8].

The handoff probability from a macrocell into one of adjacent macrocells is defined as $P_{Handoff\_MM}$, which is given by [8]

$$P_{Handoff\_MM} = \frac{\eta_{RT\_M}}{\mu + \eta_{RT\_M}}. \tag{35}$$

Active femtocell users in a macrocell can be further divided into three types of femtocell users: 1) a femtocell user with a new call in the specified macrocell, whose traffic arrival rate is λ_{FU_M}; 2) an active femtocell user handed off from a femtocell into the specified macrocell, whose traffic arrival rate is λ_{FU_FM}; 3) an active femtocell user handed off from an adjacent macrocell into the specified macrocell, whose traffic arrival rate is λ_{FU_MM}. In this case, λ_{FU_M} is expressed as

$$\lambda_{FU\_M} = NM(1-q) \cdot \lambda_F, \tag{36}$$

λ_{FU_FM} is given by

$$\lambda_{FU\_FM} = N\lambda_1 \cdot (1 - P_{FU\_F}) \cdot P_{Handoff\_FM}. \tag{37}$$

$$P_{Handoff\_MF} = \frac{A_F}{A_M} \cdot \left[\frac{\ln\left(\frac{\mu}{\eta_{RT\_M}}\right)}{\frac{\mu}{\eta_{RT\_M}}} - \frac{\eta_{RT\_M}}{\mu}\left(e^{-\frac{\eta_{RT\_M}}{\mu}} - 1\right) \right]. \tag{34}$$

$$\lambda_{FU\_MM} = (\lambda_{FU\_M} + \lambda_{FU\_FM} + \lambda_{FU\_MM}) \cdot (1 - P_{U\_M}) \cdot P_{Handoff\_MM}. \tag{38}$$

$$\lambda_{FU\_H} = \frac{1}{N}(\lambda_{FU\_M} + \lambda_{FU\_FM} + \lambda_{FU\_MM}) \cdot (1 - P_{U\_M}) \cdot P_{Handoff\_MF}, \tag{39a}$$

$$\lambda_{FU\_M} = NM(1-q) \cdot \lambda_F, \tag{39b}$$

$$\lambda_{FU\_FM} = N\lambda_1 \cdot (1 - P_{FU\_F}) \cdot P_{Handoff\_FM}, \tag{39c}$$

$$\lambda_{FU\_MM} = (\lambda_{FU\_M} + \lambda_{FU\_FM} + \lambda_{FU\_MM}) \cdot (1 - P_{U\_M}) \cdot P_{Handoff\_MM}. \tag{39d}$$

$$\lambda_{MU\_MM} = (\lambda_{MU\_M} + \lambda_{MU\_FM} + \lambda_{MU\_MM}) \cdot (1 - P_{U\_M}) \cdot P_{Handoff\_MM}. \tag{42}$$

$$\lambda_{MU\_H} = \frac{1}{N}(\lambda_{MU\_M} + \lambda_{MU\_FM} + \lambda_{MU\_MM}) \cdot (1 - P_{U\_M}) \cdot P_{Handoff\_MF}, \tag{43a}$$

$$\lambda_{MU\_M} = \left(1 - N\frac{A_F}{A_M}\right) \cdot \lambda_M, \tag{43b}$$

$$\lambda_{MU\_FM} = N\lambda_2 \cdot (1 - P_{MU\_F}) \cdot P_{Handoff\_FM}, \tag{43c}$$

$$\lambda_{MU\_MM} = (\lambda_{MU\_M} + \lambda_{MU\_FM} + \lambda_{MU\_MM}) \cdot (1 - P_{U\_M}) \cdot P_{Handoff\_MM}. \tag{43d}$$

To keep a balance in a stationary system, the outgoing traffic rate of femtocell users should be equal to the entering traffic rate of femtocell users in a macrocell [38]. Therefore, λ_{FU_MM} is given by (38).

Furthermore, the handoff-in traffic arrival rate λ_{FU_H} is derived as follows (39).

APPENDIX B

Active macrocell users in a macrocell can be further divided into three types of macrocell users: 1) a macrocell user with a new call in the specified macrocell, whose traffic arrival rate is λ_{MU_M}; 2) an active macrocell user handed off from a femtocell into the specified macrocell, whose traffic arrival rate is λ_{MU_FM}; 3) an active macrocell user handed off from an adjacent macrocell into the specified macrocell, whose traffic arrival rate is λ_{MU_MM}. In this case, λ_{MU_M} is given by

$$\lambda_{MU\_M} = \left(1 - N\frac{A_F}{A_M}\right) \cdot \lambda_M. \tag{40}$$

λ_{MU_FM} is given by

$$\lambda_{MU\_FM} = N\lambda_2 \cdot (1 - P_{MU\_F}) \cdot P_{Handoff\_FM}. \tag{41}$$

To keep a balance in a stationary system, the leaving traffic rate of macrocell users should be equal to the entering traffic rate of macrocell users in a macrocell [38]. Therefore, λ_{MU_MM} is given by (42).

Furthermore, the handoff traffic arrival rate of macrocell users λ_{MU_H} is derived by (43).

REFERENCES

[1] V. Chandrasekhar, J. G. Andrews and A. Gatherer, "Femtocell networks: a survey," *IEEE Commun. Mag.*, vol. 46, no. 9, pp. 59–67, Sept. 2008.

[2] A. Golaup, M. Mustapha and L. B. Patanapongpibul, "Femtocell access control strategy in UMTS and LTE," *IEEE Commun. Mag.*, vol. 47, no. 9, pp. 117–123, Sept. 2009.

[3] I. Humar, X. Ge, L. Xiang, M. Jo and M. Chen, "Rethinking energy-efficiency models of cellular networks with embodied energy," *IEEE Netw. Mag.*, vol. 25, no. 3, pp. 40–49, March 2011.

[4] Z. Hasan, H. Boostanimehr and V.K. Bhargava, "Green cellular networks: a survey, some research issues and challenges," *IEEE Commun. Surveys & Tutor.*, vol. 13, no. 4, pp. 524–540, Nov. 2011.

[5] Y. Chen, S. Zhang, S. Xu and G.Y. Li, "Fundamental trade-offs on green wireless networks," *IEEE Commun. Mag.*, vol. 49, no. 6, pp. 30–37, June 2011.

[6] Y. Kim, S. Lee and D. Hong, "Performance analysis of two-tier femtocell networks with outage constraints," *IEEE Trans. Wireless Commun.*, vol. 9, no. 9, pp. 2695–2700, Sept. 2010.

[7] T. Elkourdi and O. Simeone, "Femtocell as a relay: an outage analysis," *IEEE Trans. Wireless Commun.*, vol. 10, no. 12, pp. 4204–4213, Dec. 2011.

[8] Y. Zhang, "Resource sharing of completely closed access in femtocell networks," in *Proc. IEEE WCNC'10*, 2010, pp. 1–5.

[9] F. Pantisano, M. Bennis, W. Saad, and M. Debbah, "Spectrum leasing as an incentive towards uplink macrocell and femtocell cooperation," *IEEE J. Select. Areas Commun.*, vol. 30, no. 3, pp. 617–630, Apr. 2012.

[10] W. C. Cheung, T. Q. S. Quek, M. Kountouris, "Throughput optimization, spectrum allocation, and access control in two-tier femtocell networks," *IEEE J. Select. Areas Commun.*, vol. 30 , no. 3, pp. 561–574, Apr. 2012.

[11] J. Xiang, Y. Zhang, T. Skeie and L. Xie, "Downlink spectrum sharing for cognitive radio femtocell networks," *IEEE Systems Journal*, vol. 4, no. 4, pp. 524–534, Nov. 2010,

[12] D. Oh, H. Lee and Y. Lee, "Power control and beamforming for femtocells in the presence of channel uncertainty," *IEEE Trans. Veh. Technol.*, vol. 60, no. 6, pp. 2545–2554, June 2011.

[13] V. Chandrasekhar and J. G. Andrews, "Uplink capacity and interference avoidance for two-tier femtocell networks," *IEEE Trans. Wireless Commun.*, vol. 8, no. 7, pp. 3498–3509, July 2009.

[14] Y. Sun, R. P. Jover and X. Wang, "Uplink interference mitigation for OFDMA femtocell networks," *IEEE Trans. Wireless Commun.*, vol. 11, no. 2, pp. 614–625, Feb. 2012.

[15] V. Chandrasekhar, J. G. Andrews, T. Muharemovic, Z. Shen and A. Gatherer, "Power control in two-tier femtocell networks," *IEEE Trans. Wireless Commun.*, vol. 8, no. 8, pp. 4316–4328, Aug. 2009.

[16] H. Jo, C. Mun, J. Moon and J. Yook, "Interference mitigation using uplink power control for two-tier femtocell networks," *IEEE Trans. Wireless Commun.*, vol. 8, no. 10, pp. 4906–4910, Oct. 2009.

[17] P. Xia, V. Chandrasekhar and J. G. Andrews, "Open vs. closed access femtocells in the uplink," *IEEE Trans. Wireless Commun.*, vol. 9, no. 12, pp. 3798–3809, Dec. 2010.

[18] Y. Hou and D. I. Laurenson, "Energy efficiency of high QoS heterogeneous wireless communication network," in *Proc. IEEE VTC'10-Fall*, 2010, pp. 1–5.

[19] C. Khirallah, J. S. Thompson and H. Rashvand, "Energy and cost impacts of relay and femtocell deployments in long-term-evolution advanced," *IET Commun.*, vol. 5, no. 18, pp. 2617–2628, Dec. 2011.

[20] C. Han, T. Harrold, S. Armour, I. Krikidis, S. Videv, P. M. Grant, H. Haas, J. S. Thompson, I. Ku, C.-X. Wang, T. A. Le, M. R. Nakhai, J. Zhang, and L. Hanzo, "Green radio: radio techniques to enable energy efficient wireless networks," *IEEE Commun. Mag.*, vol. 49, no. 6, pp. 46–54, June 2011.

[21] K. Zhang, Y. Wang, W. Wang, M. Dohler and J. Wang, "Energy-efficiency wireless in-home: the need for interference-controlled femtocells," *IEEE Wireless Commun.*, vol. 18, no. 6, pp. 36–44, Dec. 2011.

[22] F. Cao and Z. Fan, "The tradeoff between energy efficiency and system performance of femtocell deployment," in *Proc. IEEE ISWCS'10*, 2010, pp. 315–319.

[23] A. D. Domenico, E. C. Strinati and A. Duda, "Ghost femtocells: an energy-efficiency radio resource management scheme for two-tier cellular networks," in *Proc. IEEE European Wireless'11*, 2011, pp. 1–8.

[24] L. Apio, E. Mino, L. Cucala, O. Moreno and I. Berberana, "Energy efficiency and performance in mobile networks deployments with femtocells," in *Proc. IEEE PIMRC'11*, 2011, pp. 107–111.

[25] I. Ku, C.-X. Wang, and J. S. Thompson, "The spectral, energy and economic efficiency of relay-aided cellular networks," *IET Commun.*, vol. 7, no. 14, pp. 1476–1487, Sept. 2013.

[26] X. Hong, Y. Jie, C.-X. Wang, J. Shi, and X. Ge, "Energy-spectral efficiency trade-off in virtual MIMO cellular systems," *IEEE J. Select. Areas Commun.*, vol. 31, no. 10, pp. 2128-2140, Oct. 2013.

[27] L. Hu and S. Stephen, "Personal communication systems using multiple hierarchical cellular overlays," *IEEE J. Select. Areas Commun.*, vol. 13, no. 2, pp. 406–415, Feb. 1995.

[28] S. P. Chung and M. T. Li, "Performance evaluation of hierarchical cellular CDMA networks with soft handoff queueing," *IEEE Trans. Veh. Technol.*, vol. 54, no. 2, pp. 652–672, March 2005.

[29] L. Kleinrock, *Queueing Systems*. New York, NY: John Wiley and Sons, 1975.

[30] G. Mansfield, "Femtocells in the US market–business drivers and consumer propositions," in *Proc. of the Femtocells Europe Conference*, 2008, pp. 1927–1948.

[31] C. Stuart, "Challenges facing the femtocell market–a realistic view?", in *Proc. 2nd International Conference on Home Access Points and Femtocells*, Dec. 2007.

[32] http://www.3g.co.uk/PR/July2006/3384.htm

[33] C. Bettstetter, H. Hannes, and X. Prez-Costa. "Stochastic properties of the random waypoint mobility model: epoch length, direction distribution, and cell change rate," in *Proc. the 5th ACM international workshop on modeling analysis and simulation of wireless and mobile systems*, 2002, pp. 7–14.

[34] IEEE 802.16m08/004r5, *IEEE 802.16m Evaluation Methodology Document (EMD)*, March 2009.

[35] X. Cheng, C.-X. Wang, H. Wang, X. Gao, X.-H. You, D. Yuan, B. Ai, Q. Huo, L. Song, and B. Jiao, "Cooperative MIMO channel modeling and multi-link spatial correlation properties," *IEEE J. Select. Areas Commun.*, vol. 30, no. 2, pp. 388–396, Feb. 2012.

[36] X. Ge, K. Huang, C.-X. Wang, X. Hong, and X. Yang, "Capacity analysis of a multi-cell multi-antenna cooperative cellular network with co-channel interference," *IEEE Trans. Wireless Commun.*, vol. 10, no. 10, pp. 3298–3309, Oct. 2011.

[37] http://www.femtoforum.org/

[38] Y. Lin, C. Gan and C. Liang, "Reducing call routing cost for femtocells," *IEEE Trans. Wireless Commun.*, vol. 9, no. 7, pp. 2302–2309, July 2010.